2013

Direct Solution of Current Density Induced on a Rough Surface by Forward Propagating Waves

Ramakrishna Janaswamy, *University of Massachusetts - Amherst*

Direct Solution of Current Density Induced on a Rough Surface by Forward Propagating Waves

Ramakrishna Janaswamy, *Fellow, IEEE*

***Abstract*—A new Volterra integral equation of the second kind with square integrable kernel is derived for paraxial propagation of radiowaves over a gently varying, perfectly conducting rough surface. The integral equation is solved exactly in terms of a infinite series and the necessary and sufficient conditions for the solution to exist and converge are established. Super exponential convergence of the Neumann series for arbitrary surface slope is established through asymptotic analysis. Expressions are derived for the determination of the number of terms needed to achieve a given accuracy, the latter depending on the parameters of the rough surface, the frequency of operation and the maximum range. Numerical results with truncated series are compared with that obtained by solving the integral equation numerically for a sinusoidal surface, Gaussian hill, and a random rough surface with Pierson-Moskowitz spectrum.**

***Index Terms*—Volterra Integral Equation, Parabolic Equation, Rough Surface, Irregular Terrain, Rough Sea, Small Slopes.**

I. Introduction

Wave propagation over a rough surface is a classical problem and is important in a number of areas including radar detection [1], [2], remote sensing [3], [4], wireless communications [5], [6], underwater acoustics [7] and optics [8], [9]. By rough surface we mean either a deterministic surface as in the case of an irregular terrain or a statistical one as in the case of a sea surface. Various methods such as physical optics (also known as the Kirchhoff's approximation) [10], small perturbation [9], integral equation [11], [12], [13], [14], [15], modal series [16], [17], partial differential equation [18], [19], [20], etc. are used to study scattering and propagation of waves over rough surfaces, with each offering its own niche advantage under certain situations.

When the normal distances of the source and receiving points relative to the mean surface are a small fraction of the separation between the source and observation points, and the rough surface is gently varying (meaning that its slope angles are small), propagation is primarily governed by forward traveling waves which make small angles with respect to the mean surface. Such cases are encountered, for example, in ship-ship radar/communications over a rough sea or long distance communications over irregular terrain with ground-based antennas. In such a case the Helmholtz equation, which the electromagnetic fields satisfy, may be replaced with the parabolic equation [21], wherein paraxial waves travel in a unidirectional direction with respect to one coordinate (usually range) direction. Parabolic equation and its variants has been successfully used in many propagation and bistatic scattering problems in the electromagnetics [22], acoustics [7], and optics [23] areas. The present paper is concerned with determining the current density induced on a rough surface when the fields in a semi-infinite region bounded by the rough surface satisfy the parabolic equation under time-harmonic excitation.

Integral equation methods, that make use of the Green's function for the problem at hand, are attractive owing to their ability to automatically incorporate the boundary condition at infinity with the added advantage that unknowns are distributed only on the boundary of the region of interest. In our case the boundary is simply the rough surface. Because the parabolic equation has only a first-order derivative along the range axis, the relevant integral equation will be of Volterra type as opposed to the Fredholm type [13] for the Helmholtz equation. Previous formulations of the integral equations for the parabolic equation [24], [25], [26], [27] or for low-grazing angle formulations [28] concentrated on obtaining the solution numerically using a variety of approaches. That the Volterra integral equation can be solved exactly appears to have escaped the attention of previous researchers and it is the purpose of the present paper to provide such a solution. By *exact* we mean a solution that does not involve matrix inversion, in the same sense that the infinite series solution of scattering of a perfectly conducting sphere is considered exact.

Using the Green's function for the parabolic equation, we first derive a new Volterra integral equation of the second kind in subsection II-A for the induced current density assuming a perfectly conducting rough surface and horizontal polarization. Extension to other surface types and polarizations can be carried out in a similar fashion. The kernel of the integral equation as well as the initial fields are both shown to belong to the space of square integrable functions [29]. The resulting second-kind integral equation is solved in subsection II-B exactly using Picard's method of iteration, resulting in an infinite series with iterated kernels. The necessary and sufficient conditions for the series to converge are established. An expression is found in subsection II-C for the integrated mean square error bound in terms of the maximum range, the frequency of operation and the parameters of the rough surface when the infinite series is truncated. While the exact series solution stands on its own merit, we do not claim that it will result in a numerically efficient solution for long distance propagation without further optimization of the various algorithmic steps. However, we believe that it will open the door to obtain various analytical approximations under specialized situations. For instance, the

The author is with the Department of Electrical & Computer Engineering, 100 Natural Resources Road, University of Massachusetts, Amherst, MA 01003, USA. Email: janaswamy@ecs.umass.edu.

IEEE Transactions on Antennas & Propagation, vol. 61(7), July 2013.

zeroth order approximation comprised of the right-hand side of the original integral equation is shown in subsection II-D to be accurate when the slope angles and/or the range parameters are sufficiently small. Numerical results for the current density and propagation factor obtained with a truncated series are compared in section III with those obtained on solving the integral equation numerically for a surfaces with both small and large slope angles (but still small enough so that parabolic approximation still holds). Finally, conclusions and future directions are presented in section IV. The deterministic results presented in the paper will form the starting point for the treatment of a *random* rough surface. Still, the results should have a value of their own right in areas such as wireless communication, where one is concerned with the propagation of radiowaves over a deterministic irregular terrain [30], [31], [22].

II. Theory

We consider time-harmonic propagation of two-dimensional radio waves over a 1D rough surface (a surface varying only in one direction). For simplicity, the surface is assumed to be perfectly conducting, although a similar formulation could be carried out for the more general case of an impedance surface. Fig. 1 shows the geometry of the problem along with the coordinate system assumed. All field quantities are assumed to be invariant of the y-axis and an $e^{-i\omega\tau}$ time dependence at the radian frequency $\omega = 2\pi f$ in the time variable τ is assumed and suppressed throughout. The fields are assumed to be generated by a vertically polarized magnetic source placed in the plane $x = 0$, resulting in a TE$_z$ mode with non-zero field components of E_y, H_x, and H_z, where E denotes electric field and H denotes magnetic field. The rough surface is described by $z = g(x)$ and the medium above it is assumed to be vacuum with constitutive parameters (ϵ_0, μ_0). Vacuum is treated as the limiting case of a lossy medium having wavenumber $k_0 = \omega\sqrt{\epsilon_0\mu_0}(1 + i\epsilon)$, $\epsilon > 0$, in the limit of $\epsilon \to 0$.

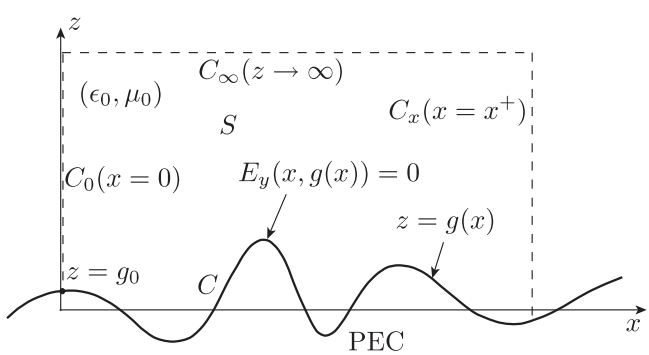

Fig. 1. A perfectly conducting rough surface bounding the region S.

We assume that the slopes of the rough surface are small enough so that back scattering can be ignored and that waves travel predominantly in the paraxial direction. In practice, waves traveling roughly within $\pm(15^o - 20^o)$ relative to the horizontal axis are correctly modeled by the formulation we are considering. The reduced field $U = e^{-ik_0x}E_y$ then satisfied the standard parabolic equation (PE) [32], [33]

$$\frac{\partial U}{\partial x} = \frac{i}{2k_0}\frac{\partial^2 U}{\partial z^2} \tag{1}$$

together with the initial condition $U(x = 0, z) = U_0(z)$ and the boundary condition $U(x, z = g(x)) = 0$. The derivation of an integral equation for the unknown surface current residing on the rough surface is facilitated by the availability of a Green's function. The Green's function, G_0, in free-space for the PE satisfies the equation

$$\frac{\partial G_0}{\partial x} = \frac{i}{2k_0}\frac{\partial^2 G_0}{\partial z^2} + \delta(x - \xi)\delta(z - \eta), \tag{2}$$

where $\delta(x)$ is the unit impulse function at $x = 0$. This linear partial differential equation with constant coefficients can be solved by employing either a Fourier transformation with respect to z [34] or a Laplace transformation with respect to x and carrying out standard manipulations. The solution is

$$G_0(x, z; \xi, \eta) = \frac{\gamma\Theta(x - \xi)}{\sqrt{x - \xi}} \exp\left[i\frac{k_0}{2}\frac{(z - \eta)^2}{(x - \xi)}\right], \tag{3}$$

where $\gamma = \sqrt{k_0/2\pi i}$ and $\Theta(x)$ is the unit step function. For later purposes the following integral representation of G_0 will become useful:

$$G_0(x, z; \xi, \eta) = \frac{\Theta(x-\xi)}{2\pi}\int_{-\infty}^{\infty} e^{ik_z(z-\eta)}e^{-i\frac{k_z^2}{2k_0}(x-\xi)}\,dk_z. \tag{4}$$

The Green's function G_0 satisfies the following basic properties:

$$\begin{aligned}
&\text{I} \quad \frac{\partial G_0}{\partial x} = -\frac{\partial G_0}{\partial \xi}, \ \frac{\partial G_0}{\partial z} = -\frac{\partial G_0}{\partial \eta}\\
&\text{II} \quad \lim_{|z|\to\infty}|G_0| = 0, \ \lim_{|z|\to\infty}|\partial G_0/\partial z| = 0\\
&\text{III} \quad \lim_{x\to\xi} G_0(x, z; \xi, \eta) = \delta(z - \eta)\\
&\text{IV} \quad \lim_{z\to\eta}\frac{i}{2k_0}\frac{\partial G_0}{\partial z} = -\text{Sign}(z - \eta)\frac{1}{2}\delta(x - \xi)
\end{aligned}$$

as can be easily verified by keeping in mind that k_0 has a vanishingly small positive imaginary part.

A. Volterra Integral Equation of the Second Kind

Consider a region S bounded by $C_0 + C + C_x + C_\infty$ as shown in Fig. 1. The contour C_0 is defined by the vertical line $x = 0$, C_x is defined by the line $x = x^+$, C_∞ is defined by the horizontal line $z \to \infty$ and C corresponds to the rough surface. Integrating the null quantity $\{G_0 \cdot [\partial U/\partial\xi - (i/2k_0)\partial^2 U/\partial\eta^2] + U \cdot [\partial G_0/\partial\xi + (i/2k_0)\partial^2 G_0/\partial\eta^2 + \delta(x - \xi)\delta(z - \eta)]\}$ over S and assuming that U and $\partial U/\partial z$ are bounded at infinity, it can be shown by making use of the properties (I)-(IV) of the Green's function

that

$$U(x,z) = \int_{g_0}^{\infty} U_0(\eta) G_0(x,z;0,\eta)\, d\eta - \frac{i}{2k_0}\int_0^x J(\xi) G_0[x,z;\xi,g(\xi)]\, d\xi, \quad (5)$$

$$=: U_i(x,z) + U_s(x,z) \quad (6)$$

where $g_0 = g(x=0)$ and $J(\xi) := \frac{\partial U}{\partial \eta}[\xi, \eta = g(\xi)]$ is referred to as the *current density*[1]. The first integral on the right hand side of (5) constitutes the field in free-space, $U_i(x,z)$, that arises from the initial field $U_0(\eta)$, and the second term corresponds to the scattered field, $U_s(x,z)$, that is generated by the vertical derivative $\partial U/\partial z$ of the reduced field residing on C.

An integral equation of the first kind can be derived as in [27] by taking the limit as $z \to g(x)$ along a vertical line and making use of the fact that $U(x, g(x)) = 0$. However, we are interested in deriving an integral equation of the second kind so that an analytical solution in terms of an infinite series is possible. To this end, we take the vertical derivative on both sides of (5) and take the limit as $z \to g(x)$ on a vertical line. The following limit relation is encountered, which can be easily derived based on property (IV) of G_0:

$$\lim_{z\to g(x)} \frac{1}{ik_0}\frac{\partial G_0}{\partial z}[x,z;\xi,g(\xi)] = \delta(x-\xi) + g_d(x;\xi)\cdot G_0[x,g(x);\xi,g(\xi)] \quad (7)$$

where

$$g_d(x;\xi) := \frac{g(x)-g(\xi)}{x-\xi}. \quad (8)$$

The function $g_d(x;\xi)$ is bounded when the slopes of the rough surface are finite. Using (7), the following Volterra integral equation of the second kind in the unknown $J(x)$ is obtained from (6):

$$J(x) - \gamma \int_0^x \frac{K_0(x;\xi)}{\sqrt{x-\xi}} J(\xi)\, d\xi = J_i(x), \quad (9)$$

where

$$K_0(x;\xi) := g_d(x;\xi) e^{ik_0(x-\xi)g_d^2(x;\xi)/2} = K_0^*(\xi;x), \quad (10)$$

with superscript $*$ denoting complex conjugate and

$$J_i(x) := -2\int_{g_0}^{\infty} U_0(\eta)\frac{\partial G_0(x,g(x);0,\eta)}{\partial \eta}\, d\eta \quad (11)$$

$$= 2\int_{g_0}^{\infty} \frac{\partial U_0}{\partial \eta} G_0(x,g(x);0,\eta)\, d\eta \quad (12)$$

[1]It may be noted that the traditional current density for 2D propagation defined as $\boldsymbol{y}\cdot(\boldsymbol{n}\times\boldsymbol{H})$ can be approximately related to the vertical derivative for surfaces having small slopes by noting that $\boldsymbol{y}\cdot(\boldsymbol{n}\times\boldsymbol{H}) = (i/\omega\mu_0)\boldsymbol{n}\cdot\nabla E_y = (i/\omega\mu_0)[\partial E_y/\partial z - g'(x)\partial E_y/\partial x]/\sqrt{1+(g'(x))^2} \approx (i/\omega\mu_0)\partial E_y/\partial z/\sqrt{1+(g'(x))^2} = (i/\omega\mu_0)e^{ik_0x}J(x)/\sqrt{1+(g'(x))^2}$, where $g'(x)$ is the derivative of $g(x)$.

is the incident current density defined entirely in terms of the initial data. The latter equality in (12) assumes that the initial data is differentiable. Equation (9) was used in [26] and [35] and solved numerically, although its derivation was not shown there. The auxiliary kernel $K_0(x;\xi)$ will be bounded if Lipschitz conditions are imposed on the function $g(x)$ describing the rough surface. This will be clarified in subsection II-B. Note that for a differentiable rough surface, $g_d(x;x) = g_d(x;x^-) = g'(x)$ and $K_0(x;x) = g'(x)$. A Volterra integral equation of the second kind based on the parabolic approximation and different from (9) was also given in [24], [25] for the attenuation function over a lossy irregular terrain. Most previous works in radiowave and acoustic propagation, including [26], [27] and [25], were concerned with obtaining a numerical solution of the derived integral equations. Our goal, however, is to obtain a direct solution that will not involve matrix inversions.

The kernel of the integral equation in (9) has a weak singularity as evidenced by the presence of $\sqrt{x-\xi}$ in the denominator of the integrand. This will prevent a direct application of the theory for $\mathcal{L}_2(0,X)$ kernels (*i.e.* square integrable over a finite range $x = X$) available in standard references such as [36]. We will first transform it to another integral equation with a square integrable kernel using the device suggested in [36]. We rewrite (9) as

$$\gamma \int_{t=0}^{x'} \frac{K_0(x';t)}{\sqrt{x'-t}} J(t)\, dt = J(x') - J_i(x'), \quad (13)$$

multiply both sides with $\gamma K_0(x;x')/\sqrt{x-x'}$ and integrate over $x' = (0,x)$. The two integrals on the left hand side may be interchanged by noting that

$$\int_{x'=0}^{x} dx' \int_{t=0}^{x'} dt = \int_{t=0}^{x} dt \int_{x'=t}^{x} dx'. \quad (14)$$

Equation (13) is again utilized on the right hand side of the resulting equation to finally yield the following Volterra integral equation of the second kind with a square integrable kernel K_1:

$$J(x) - \gamma^2 \int_{t=0}^{x} K_1(x;t) J(t)\, dt = J^{(0)}(x) \quad (15)$$

where

$$J^{(0)}(x) := J_i(x) + \gamma \int_{x'=0}^{x} J_i(x') \frac{K_0(x;x')}{\sqrt{x-x'}}\, dx', \quad (16)$$

and

$$K_1(x;t) := \int_{x'=t}^{x} \frac{K_0(x;x')K_0(x';t)}{\sqrt{(x-x')(x'-t)}}\, dx'. \quad (17)$$

The kernel K_1 is actually bounded in addition to being in $\mathcal{L}_2(0,X)$ space. The weak singularity in the integrand of (17) is removable as can be seen by making the change of variable

$x' = x\sin^2\theta + t\cos^2\theta$ to result in

$$K_1(x;t) = 2\int_{\theta=0}^{\pi/2} K_0(x; x\sin^2\theta + t\cos^2\theta) \times K_0(x\sin^2\theta + t\cos^2\theta; t)\, d\theta, \quad (18)$$

which shows that K_1 is bounded if $K_0(x;x')$ is bounded. Equation (18) also shows that $K_1(x,x) = \pi K_0^2(x;x) = \pi[g'(x)]^2$. The transformation $x' = x\sin^2\theta$ in (16) yields the expression

$$J^{(0)}(x) = J_i(x) + 2\gamma\sqrt{x} \times \int_{\theta=0}^{\pi/2} J_i(x\sin^2\theta) K_0(x; x\sin^2\theta)\sin\theta\, d\theta, \quad (19)$$

which reveals that $J^{(0)}(x)$ is bounded and square integrable in $(0,X)$ if $J_i(x)$ is bounded.

B. Exact Current Distribution

Under certain conditions, the integral equation (15) can be readily solved by the Picard's method of successive approximation to result in an infinite series, also known as the *Neumann series* [36]. We assume at the outset that the initial data is such that the incident current density $J_i(x)$ is bounded. A *sufficient condition* for $|J_i(x)|$ to be bounded can be established by making use of (11) and (4). Using the Fourier representation (4) of the Green's function in (11), we see that

$$\begin{aligned} J_i(x) &= \frac{i}{\pi}\int_{g_0}^{\infty}\int_{-\infty}^{\infty} U_0(\eta) k_z e^{ik_z(g(x)-\eta)} e^{-ik_z^2 x/2k_0}\, dk_z d\eta \\ &= \frac{i}{\pi}\int_{-\infty}^{\infty} k_z \overline{U}_0(k_z) e^{ik_z g(x)} e^{-ik_z^2 x/2k_0}\, dk_z, \end{aligned} \quad (20)$$

where $\overline{U}_0(k_z) = \int_{g_0}^{\infty} U_0(\eta)\exp(-ik_z\eta)\, d\eta$ is the Fourier transform of $U_0(\eta)$. Therefore,

$$\pi|J_i(x)| \le \int_{-\infty}^{\infty} \left|k_z \overline{U}_0(k_z)\right| dk_z. \quad (21)$$

The integrand of the right hand side is recognized as the modulus of the Fourier spectrum of $dU_0(\eta)/d\eta$. Thus, (21) implies that a sufficient condition for $J_i(x)$ to be bounded is the existence of the first derivative of $U_0(\eta)$ in the entire interval (g_0,∞). However, $J_i(x)$ can remain finite even if $U_0(\eta)$ is discontinuous at finite number of isolated points. This is certainly true for a truncated Gaussian type of source that is commonly used in propagation studies [18]. Indeed, for a Guassian source of amplitude A, centered at H_t with a standard deviation σ_z and truncated to zero below $\eta = g_0$,

$$U_0(\eta) = \frac{A}{\sqrt{2\pi}\sigma_z} e^{-(\eta-H_t)^2/2\sigma_z^2}, \quad \eta = (g_0^+, \infty), \quad (22)$$

and we get

$$J_i(x) = \frac{A\left[H_t - g(x)\right]}{\left(\sigma_z^2 + ix/k_0\right)^{3/2}}\sqrt{\frac{2}{\pi}} f_i \times \exp\left[-\frac{(H_t - g(x))^2}{2\left(\sigma_z^2 + ix/k_0\right)}\right] \quad (23)$$

where

$$\begin{aligned} f_i &= 1 - \frac{1}{2}\mathrm{erfc}\left(\gamma_g\sqrt{\beta} + \frac{u_0}{2\sqrt{\beta}}\right) + \\ &\quad + \frac{\exp\left[-\left(\gamma_g\sqrt{\beta} + \frac{u_0}{2\sqrt{\beta}}\right)^2\right]}{2\gamma\sqrt{\pi\beta}} \quad (24) \\ &\sim 1, \quad u_0 >> 1 \quad (25) \end{aligned}$$

with $u_0 = (H_t - g_0)/\sigma_z$, $\gamma_g = ik_0(H_t - g(x))\sigma_z/x$, $(2\beta)^{-1} = (1 - ik_0\sigma_z^2/x)$ and $\mathrm{erfc}(\cdot)$ denotes complementary error function [37]. Hence $J_i(x)$ is bounded for any x in a finite range $(0,X)$ even though $U_0(g_0^+) \neq 0$ and $U_0(g_0)$ is set to zero.

We next assume that the function defining the rough surface satisfies the Lipschitz's condition [29] on $(0,X)$, *i.e.*, for a positive constant α_g

$$|g(x) - g(\xi)| \le \alpha_g |x - \xi|. \quad (26)$$

Lipschitz requirement is stronger than continuity, but weaker than differentiability. For differentiable functions, α_g is simply the maximum absolute derivative, but the Lipschitz condition is satisfied also by non-differentiable functions. For instance, a continuous, piecewise linear rough surface satisfies the Lipschitz condition with $\alpha_g = \max(\text{absolute slope})$. Thus the function in (8) satisfies $|g_d(x;\xi)| \le \alpha_g$ and the kernel in (10) remains bounded: $|K_0(x;\xi)| \le \alpha_g$. As already pointed out in subsection II-A, the kernel $K_1(x;t)$ and the function $J^{(0)}(x)$ are both bounded and hence belong to the $\mathcal{L}_2(0,X)$ space if $K_0(x;x')$ and $J_i(x)$ are respectively bounded. In view of these results, the following theorem [36], [38] immediately applies to our situation:

Theorem (Volterra Integral Equation of the Second Kind)**.** *The Volterra integral equation of the second kind (15), where the kernel $K_1(x;t)$ and the function $J^{(0)}(x)$ belong to the class $\mathcal{L}_2(0,X)$, has a unique non-trivial solution in $\mathcal{L}_2(0,X)$ for arbitrary $\gamma \in \mathbb{C}$. This solution is given by the formula*

$$J(x) = J^{(0)}(x) + \sum_{n=1}^{\infty}\gamma^{2n}\int_0^x K_n(x;t) J^{(0)}(t)\, dt, \quad (27)$$

where the kernels $K_n(x;t)$ satisfy the recurrence relation

$$K_n(x;t) = \int_{\xi=t}^{x} K_1(x;\xi) K_{n-1}(\xi;t)\, d\xi, \text{ for } n \ge 2. \quad (28)$$

It is important to bear in mind that for any $n = 1, 2, \ldots$, $K_n(x;t) = 0$ for $t > x$. Computation of the solution from (27) requires (i) determining the zeroth order current density $J^{(0)}(x)$ from (16) and (ii) determining the kernels $K_n(x;t)$ by

evaluating the integrals (28), and (iii) evaluating the integrals on the right hand side of (27). The amount of computational labor depends on the number of terms used in the series, the nature of the rough surface, the maximum range X, and the integration scheme employed.

C. Truncated Series and Error Estimates

In practice one would like to truncate the series in (27) to some finite upper limit to aid computation. Our main goal in this subsection is to investigate the rate at which the truncated series solution approaches the exact solution as the number of terms is increased. Using asymptotic theory we show that the truncation limit can be chosen appropriately so that the error with respect to the exact solution can be made as small as desired for *any* slope (of course within the constraints imposed by the validity of the parabolic approximation). We also derive an expression for the integrated root mean square error as a function of the physical parameters of the problem as well as expressions for the determination of the number of terms needed to achieve a given accuracy. We make repeated use of the Schwartz inequality [29], which states for two complex valued functions $f_1(x)$ and $f_2(x)$ in $x \in (a,b)$ that

$$\left| \int_a^b f_1(x) f_2(x)\, dx \right|^2 \leq \int_a^b |f_1(x)|^2\, dx \int_a^b |f_2(x)|^2\, dx. \quad (29)$$

The $\mathcal{L}_2$ norm of the nth iterate, $\|J^{(n)}\|$, over the domain $x \in (0,X)$ is defined as

$$\|J^{(n)}(x)\|^2 = \int_0^X \left| J^{(n)}(x) \right|^2 dx. \quad (30)$$

The Nth iterate of the current density is that which is obtained by truncating the upper limit in the right hand of (27) to N:

$$\begin{aligned} J^{(N)}(x) &= J^{(0)}(x) + \sum_{n=1}^{N} \gamma^{2n} \int_0^x K_n(x;t) J^{(0)}(t)\, dt \\ &\equiv J^{(0)}(x) + \sum_{n=1}^{N} \left[J^{(n)}(x) - J^{(n-1)}(x) \right], \quad (31) \end{aligned}$$

where the incremental contribution of the nth term in the summation is

$$J^{(n)}(x) - J^{(n-1)}(x) = \left(\frac{-i}{\lambda} \right)^n \int_0^x K_n(x;t) J^{(0)}(t)\, dt \quad (32)$$

on recognizing that $\gamma^2 = -i/\lambda$, where λ is the free-space wavelength. For N sufficiently large, $J^{(N)}(x)$ will be close to the exact solution $J(x) \equiv J^{(\infty)}(x)$. For a given accuracy, that value of N depends on the maximum range $x = X$, the nature of the rough surface, frequency of operation, etc.

We will first provide worst-case estimates for the error incurred in employing the Nth iterate by performing an analysis along the lines of Tricomi [36]. From subsections II-A and II-B we can conclude that

$$\begin{aligned} |K_0(x;t)| &\leq \alpha_g, \text{ and} \quad (33) \\ |K_1(x;t)| &\leq \pi \alpha_g^2. \quad (34) \end{aligned}$$

It is also clear from observing the phase of K_0 in equation (10) that the maximum effective wavenumber of oscillation along the terrain is $k_x = k_0 \alpha_g^2/2$ and the corresponding minimum wavelength of oscillation is $\lambda_x = 2\pi/k_x = 2\lambda/\alpha_g^2$. Hence, if the maximum slope angle of the terrain is 10°, the minimum wavelength of oscillation is $\lambda_x \approx 64\lambda$. The squared norm of the kernel $K_n(x;t)$ is defined as

$$\|K_n\|^2 = \int_{x=0}^{X} \int_{t=0}^{x} |K_n(x;t)|^2\, dt\, dx. \quad (35)$$

Let us designate

$$\begin{aligned} A^2(x) &= \int_{t=0}^{X} |K_1(x;t)|^2\, dt, \quad 0 \leq x \leq X \\ &= \int_{t=0}^{x} |K_1(x;t)|^2\, dt \leq (\pi \alpha_g^2)^2 x, \quad (36) \end{aligned}$$

and

$$\begin{aligned} B^2(t) &= \int_{x=0}^{X} |K_1(x;t)|^2\, dx, \quad 0 \leq t \leq X \\ &= \int_{x=t}^{X} |K_1(x;t)|^2\, dx \leq (\pi \alpha_g^2)^2 (X-t), \quad (37) \end{aligned}$$

where the last inequalities in (36) and (37) follow from (33) and (34) respectively. Using these it is easy to see that

$$\begin{aligned} \|K_1\|^2 &= \int_{x=0}^{X} A^2(x)\, dx = \int_{t=0}^{X} B^2(t)\, dt \quad (38) \\ &\leq \left(\pi \alpha_g^2 X \right)^2 / 2. \quad (39) \end{aligned}$$

From the upper bound in (39) one can conclude that $\|K_1\|$ increases linearly with X and quadratically with α_g. It is straightforward to show that all the higher order kernels are also bounded. Schwartz inequality applied to (28) yields the inequalities

$$\|K_n\| \leq \|K_1\| \cdot \|K_{n-1}\| \Longrightarrow \|K_n\| \leq \|K_1\|^n, \; n \geq 1. \quad (40)$$

However, it is possible to get tighter bounds on the norms using the procedure outlined in [36] so that the convergence of the series (27) can be established for arbitrary surface slope and

maximum range. Now

$$\begin{aligned} |K_2(x;t)|^2 &= \left| \int_{\xi=t}^{x} K_1(x;\xi)K_1(\xi;t)\,d\xi \right|^2 \\ &\le \int_{\xi=0}^{X} |K_1(x;\xi)|^2\,d\xi \cdot \int_{\xi=0}^{X} |K_1(\xi;t)|^2\,d\xi \\ &\le A^2(x)B^2(t) \end{aligned} \tag{41}$$

Similarly, it can be shown that

$$|K_{n+2}(x;t)|^2 \le A^2(x)B^2(t)F_n(x;t), n = 0, 1, \ldots, \tag{42}$$

where $F_0(x;t) := 1$ and

$$F_n(x;t) = \int_{\xi=t}^{x} A^2(\xi)F_{n-1}(\xi;t)\,d\xi, n = 1, 2, \ldots. \tag{43}$$

On realizing that $A^2(x) = \partial F_1(x;t)/\partial x$, one can show that

$$F_n(x;t) = \frac{F_1^n(x;t)}{n!}. \tag{44}$$

Now

$$F_1(x;t) = \int_{\xi=t}^{x} A^2(\xi)\,d\xi \le \int_{\xi=0}^{X} A^2(\xi)\,d\xi = \|K_1\|^2. \tag{45}$$

Using (45) and (44) in (42), we arrive at

$$|K_{n+2}(x;t)|^2 \le A^2(x)B^2(t)\frac{\|K_1\|^{2n}}{n!}, n = 0, 1, \ldots, \tag{46}$$

which implies that for $n \ge 2$

$$\|K_n\| \le \frac{\|K_1\|^n}{\sqrt{(n-2)!}}, \tag{47}$$

which is a substantial improvement over the bounds expressed by (40). Consider the local mean square error incurred in truncating the series to $N = M + 1$ terms, $M \ge 0$:

$$\begin{aligned} I_\epsilon^2(x) &= \left| J^{(\infty)}(x) - J^{(N)}(x) \right|^2 \\ &= \left| \sum_{n=N+1}^{\infty} \left(\frac{-i}{\lambda}\right)^n \int_{t=0}^{x} K_n(x;t)J^{(0)}(t)\,dt \right|^2 \\ &\le \sum_{n=N+1}^{\infty} \frac{1}{\lambda^{2n}} \int_{t=0}^{x} |K_n(x;t)|^2\,dt \int_{t=0}^{x} \left|J^{(0)}(t)\right|^2 dt \\ &= \|J^{(0)}\|^2 \sum_{n=N+1}^{\infty} \frac{1}{\lambda^{2n}} \int_{t=0}^{x} |K_n(x;t)|^2\,dt. \end{aligned} \tag{48}$$

Defining $\rho = (\|K_1\|/\lambda)^2$, the relative integrated mean square error is

$$\begin{aligned} \epsilon^2(N) &= \frac{1}{\|J^{(0)}\|^2} \int_{x=0}^{X} I_\epsilon^2(x)\,dx \\ &\le \sum_{n=N+1}^{\infty} \frac{1}{\lambda^{2n}} \int_{x=0}^{X} \int_{t=0}^{x} |K_n(x;t)|^2\,dt\,dx \\ &= \sum_{n=N+1}^{\infty} \frac{\|K_n\|^2}{\lambda^{2n}} \qquad (49) \\ &\le \sum_{n=N+1}^{\infty} \frac{1}{\lambda^{2n}} \frac{\|K_1\|^{2n}}{(n-2)!} \qquad (50) \\ &= \rho^2 \sum_{m=M}^{\infty} \frac{\rho^m}{m!} = \rho^2 e^\rho P(M,\rho), \qquad (51) \end{aligned}$$

where the function $P(M,\rho)$ is related to the lower incomplete gamma function $\gamma(M,\rho)$ [37] as $P(M,\rho) = \gamma(M,\rho)/\Gamma(M)$. It is clear from (51) that the error tends to zero as $M \to \infty$ for any finite ρ. However, to gain more insight into the convergence process such as the rate of decay at infinity, it is necessary to examine how the error behaves for large M. A uniform asymptotic form of the function P for large M is available in [39]:

$$P(M,\rho) \sim \frac{1}{2}\mathrm{erfc}(-\eta\sqrt{M/2}), \quad M \gg 1 \tag{52}$$

where $\eta^2 = 2(a - \ln(ae))$, $\mathrm{sign}(\eta) = \mathrm{sign}(a-1)$ and $a = \rho/M$. For $M \gg \rho$, $a \to 0$ and $\eta \sim -\sqrt{2\ln(M/e\rho)}$. Using the asymptotic form of the complementary error function, $\mathrm{erfc}(z) \sim \exp(-z^2)/\sqrt{2\pi}z$ for large $|z|$, we can conclude that $\mathrm{erfc}(-\eta\sqrt{M/2}) < (e\rho/M)^M/\sqrt{2\pi M\log(M/e\rho)}$. Inserting this in (52) we get

$$\epsilon^2(N) < \frac{\rho^2 e^\rho}{2\sqrt{\pi M \ln(M/e\rho)}} \left(\frac{e\rho}{M}\right)^M, \; M > e\rho, M \gg 1, \tag{53}$$

which clearly decays to zero *super-exponentially* as $M \to \infty$ for *any* finite ρ. The same right hand side as in (53) is obtained if one starts from (50) and makes use of $(m+M)! > m!\,M!$ and the lower bound for $M!$ (see formula (6.1.38) of [37]).

Having established that the Neumann series converges to the exact solution for any slope and range, it is of interest to determine the order N for which the current density achieves a given accuracy. To this end, we first note from (31) and (32) that

$$\begin{aligned} \|J^{(N)}\|^2 &\le \|J^{(0)}\|^2 + \sum_{n=1}^{N} \int_{0}^{X} \left|J^{(n)}(x) - J^{(n-1)}(x)\right|^2 dx \\ &\le \|J^{(0)}\|^2 \left[1 + \sum_{n=1}^{N} \frac{\|K_n\|^2}{\lambda^{2n}}\right]. \end{aligned} \tag{54}$$

Similarly,

$$\|J^{(\infty)}\|^2 \le \|J^{(0)}\|^2 \left[1 + \sum_{n=1}^{\infty} \frac{\|K_n\|^2}{\lambda^{2n}}\right]. \tag{55}$$

To achieve a relative accuracy of $(1-\delta)$ (or a relative error of δ), where $\delta \ll 1$, in the current distribution, we set $\|J^{(N)}\|^2 = (1-\delta)^2\|J^{(\infty)}\|^2 \approx (1-2\delta)\|J^{(\infty)}\|^2$. It is reasonable to use upper limits for $\|J^{(N)}\|$ and $\|J^{(\infty)}\|$ as given by (54) and (55) as both are based on the same kind of approximations. Hence we get

$$\sum_{n=N+1}^{\infty} \frac{\|K_n\|^2}{\lambda^{2n}} = 2\delta\left(1+\sum_{n=1}^{\infty}\frac{\|K_n\|^2}{\lambda^{2n}}\right). \tag{56}$$

The upper limit in both summations may be replaced with a large integer $N_{\max}$ without causing too much error. We then get a form more suitable for numerical computations as

$$F(N,N_{\max}) := \sum_{n=N+1}^{N_{\max}} \frac{\|K_n\|^2}{\lambda^{2n}} = 2\delta\left(1+\sum_{n=1}^{N_{\max}}\frac{\|K_n\|^2}{\lambda^{2n}}\right) =: G. \tag{57}$$

When the current density is accurately represented by the Nth iterate, the left hand side of (56) may be approximated by the first term in the series to result in the following useful formula for determining N:

$$F(N,N+1) = \frac{\|K_{N+1}\|^2}{\lambda^{2(N+1)}} \approx G. \tag{58}$$

For a given rough surface, maximum range, and frequency of operation, the various $\|K_n\|$ may be computed and N determined from (57) or (58) to achieve a specified relative error δ. From (47) and (39), it is clear that all of the norms can increase linearly with maximum range and quadratically with the maximum absolute slope angle. Hence the number of terms N is expected to increase with the maximum absolute slope angle of the surface, the maximum range and the frequency of operation. Conversely, for a shallow rough surface, or small ranges or low frequencies, few terms in the series should be adequate.

D. Accuracy of the Zeroth Order Approximation

The zeroth order approximation to the current density, $J^{(0)}(x)$, given in (16), itself may be adequate when the range and/or the terrain slopes are small so that $\rho \ll 1$. Note that the zeroth order approximation is dependent on the initial field $U_0(z)$ via the incident current density, $J_i(x)$, as well as on the properties of the rough surface. Indeed, it is itself the first-order iterate of the original integral equation (9). This is in contrast to the normal physical optics approximation [10], [12] wherein the zeroth order term primarily involves evaluation of the tangential component of the incident magnetic field along the rough surface. Using the upper bound for $\|K_1\|$ from (39) and by arbitrarily setting $\rho \le 1/\pi^3$, one may conclude that if $\alpha_g^2 X/\lambda \le \sqrt{2}/\pi^{5/2}$, the current density will be dominated by the zeroth order approximation. In other words, the zeroth order approximation is good for a maximum range up to about

$$X = X_0 = \frac{\sqrt{2}\lambda}{\alpha_g^2\pi^{5/2}}, \tag{59}$$

which varies inversely with α_g^2. If the slope angle is doubled, the corresponding maximum range up to which the zeroth order approximation is accurate decreases by a factor of four. The maximum range is also seen to increase linearly with wavelength of operation. All else being equal, a decrease in frequency of operation by a factor of two increases the maximum range by a factor of two. The zeroth order approximation should consequently be very good for low frequencies and small slope angles.

III. Numerical Results for Truncated Series

The exact solution for the current density $J(x)$ is given in (27) with the iterated kernels defined by (28) and the zeroth order current density given in (16). The substitution $\xi = x\sin^2\theta + t\cos^2\theta$ reveals that the nth iterated kernel $K_n(x;t)$ is a smooth function of both arguments and behaves as $(x-t)^{n-1}$ near the boundaries. It may be noted that the purpose of the paper is not to offer the exact solution as a numerically efficient solution for long ranges and no effort was spent on numerically optimizing the series solution. Notwithstanding this, the numerical computation of the various kernels can be carried out using any of the standard integration routines. As remarked in subsection II-C, the relative error in the truncated series for a given N depends on the wavelength λ, Lipschitz constant α_g, the maximum range X. We compare the performance of the approximate solution (31) with that obtained by solving the integral equation (9) numerically following the procedure outlined in [26]. The latter solution was obtained with a range discretization of Δx and we label it as J_{num} in the plots. We also compute the total field on a vertical line at $x = X$ using (6) and plot the propagation factor $PF = \left|U(X,z)/U^i(X,z)\right| = |1+U_s(X,z)/U_i(X,z)|$ obtained by using both the numerical solution $J_{\text{num}}(x)$ and $J^{(N)}(x)$. Two extreme examples are considered first, one having a relatively large slope angle and a second having a relatively long range. Even though the Neumann series solution converges for any slope angle, one has to keep in mind that the parabolic equation approximation itself will break down if the absolute slope angles are greater than roughly 7.5^o or so. We also show results for propagation of low-grazing angles waves over one realization of random sea surface, whose roughness spectrum is modeled by the Pierson-Moskowitz spectrum [40].

The first example we consider is a rough surface characterized by $g(x) = A_{pp}\sin^2(\pi x/L)$. The slope of this surface is $(A_{pp}\pi/L)\sin(2\pi x/L)$ yielding $\alpha_g = \pi A_{pp}/L$. We use $A_{pp} = 1\,\text{m}$, $L = 30\,\text{m}$ to result in $\alpha_g = 0.1051$. The maximum absolute slope angle with these parameters is 6°. A Gaussian source of the form (22) with $\sigma_z = 4\lambda/3$, $H_t = 5\,\text{m}$ and operating at a frequency $f = 1\,\text{GHz}$ ($\lambda = 0.3\,\text{m}$) was used for the initial source and the current density was calculated until a range $X = 300\,\text{m}$. For these parameters, $\|K_1\|/\lambda \approx 3.56$, $\rho \approx 12.7$, and $X_0 \approx 2.2\,\text{m}$. The numerical solution $J_{\text{num}}(x)$ was obtained using $\Delta x = 0.5\,\text{m} = 5\lambda/3$. Recall from subsection II-C that the minimum effective wavelength along the surface is $\lambda_x = 2\lambda/\alpha_g^2 \approx 181\lambda$ here. Hence the step size of $\Delta x = 5\lambda/3$ is a small fraction of this minimum wavelength and should be more than adequate to sample the current density along the surface. Fig. 2 shows the upper bound to the root mean square (RMS) error $\epsilon(N)$ as given by (49), versus N. The RMS error computed

directly by using the various iterates of the current density

$$\epsilon_{\rm num}(N) = \sqrt{\frac{\int_0^X |J^{(N)}(x) - J^{(N_{\rm max})}(x)|^2\,dx}{\int_0^X |J^{(0)}(x)|^2\,dx}} \qquad (60)$$

is also shown in the figure for $N_{\rm max} = 30$, where $J^{(N_{\rm max})}(x)$ may be roughly regarded as the exact current distribution. Both curves are seen to have nearly the same asymptotic slope and suggest that with $N \approx 5-8$ terms, the relative error will be *less than* 10^{-2}. Fig. 3 shows the curves $F(N, N_{\rm max})$ and $F(N, N+1)$ in (57) and (58), respectively, versus N and their intersection with the quantity G for an accuracy of $(1-\delta)$ = 99.99%. It is seen that $N \approx 5$ in agreement with the estimate obtained from Fig. 2. Fig. 4 shows the magnitude of current density $J^{(N)}(x)$ for $N = 0$, $N = 5$ together with $J_{\rm num}(x)$. Clearly, the zeroth order approximation is inadequate for these parameters and the $N = 5$ solution remains very close to $J_{\rm num}(x)$. Fig. 5 shows that the propagation factor calculated with $J^{(5)}(x)$ agrees very well with that obtained with $J_{\rm num}(x)$.

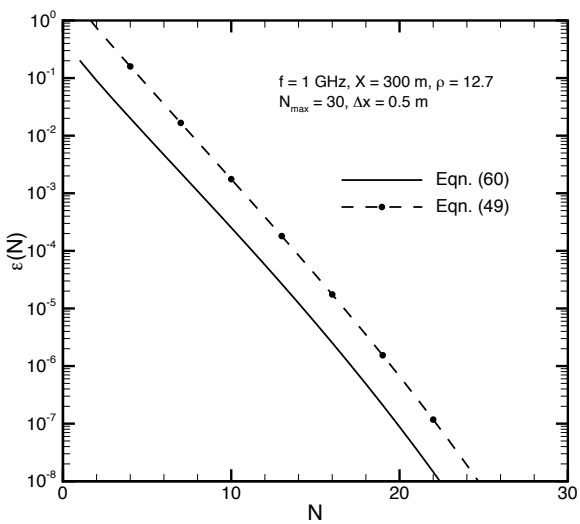

Fig. 2. Upper bound to the RMS error versus N for a sinusoidal rough surface $g(x) = A_{pp}\sin^2(\pi x/L)$.

Equation (57) predicts that for a given relative accuracy, frequency of operation and maximum slope, the number of terms increases with the maximum range X. The increase with X is, however, not linear. We have confirmed this through numerical computations. For instance, for a sinusoidal surface with a maximum slope angle of 6° and $L = 3\,$m, we observed that $N = 1$ terms as calculated from (57) gave accurate results for the current distribution when $X = 30\,$m, whereas $N = 2$ terms were required for $X = 300\,$m to achieve the same relative accuracy.

The second example we choose is that of propagation over a gaussian hill defined by $g(x) = A_{pp}\exp\left(-(x-L)^2/\sigma_x^2\right)$. The maximum absolute slope of the gaussian hill appears at $x = L \pm \sigma_x$ and takes the value $\sqrt{e}A_{pp}/\sigma_x = \alpha_g$. We choose $A_{pp} = 5\,$m, $L = 1.5\,$km, $\sigma_x = 0.5\,$km. The source

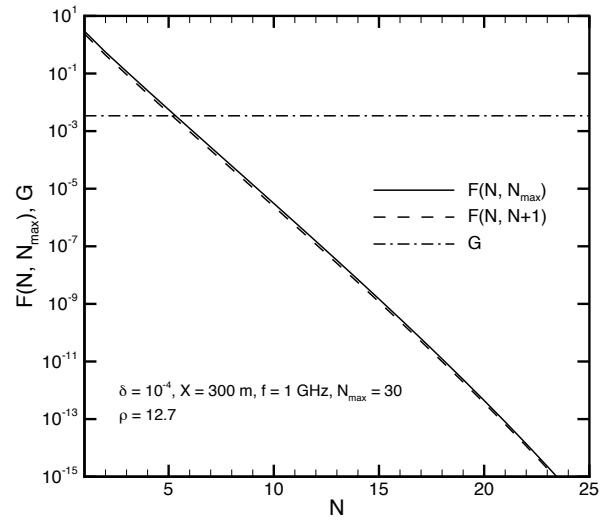

Fig. 3. Curves for the determination of number of terms needed for a specified accuracy for a sinusoidal rough surface $g(x) = A_{pp}\sin^2(\pi x/L)$.

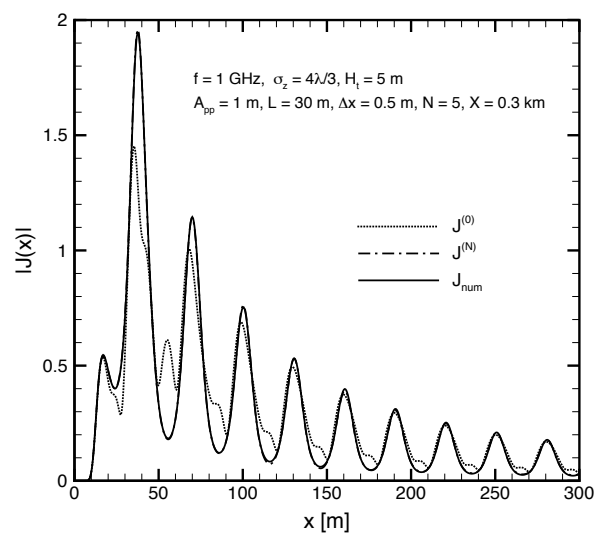

Fig. 4. Modulus of current density on a sinusoidal rough surface $g(x) = A_{pp}\sin^2(\pi x/L)$.

parameters were the same as in the previous example except that $H_t = 2\,$m. For these parameters, $\alpha_g = 6.0653 \times 10^{-3}$, $\|K_1\|/\lambda \approx 0.2952$, $\rho \approx 0.087$, and $X_0 \approx 660\,$m. The maximum absolute slope angle in this case equals 0.35^o. The numerical solution was computed with $\Delta x = 6\,$m. The modulus of the current density is shown in Fig. 6 for $N = 0$ and $N = 1$ along with the numerical solution. The $N = 2$ solution, not shown here, was virtually indistinguishable from the numerical solution over the four orders of magnitude shown in Fig. 6. It is also

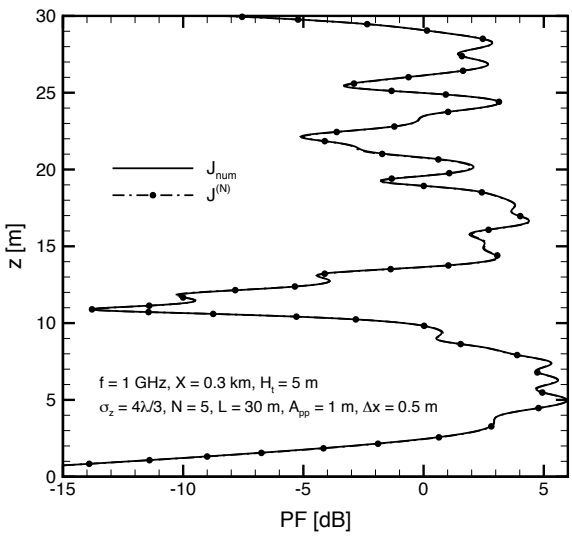

Fig. 5. Propagation factor at $X = 300\,\mathrm{m}$ for the sinusoidal rough surface $g(x) = A_{pp}\sin^2(\pi x/L)$.

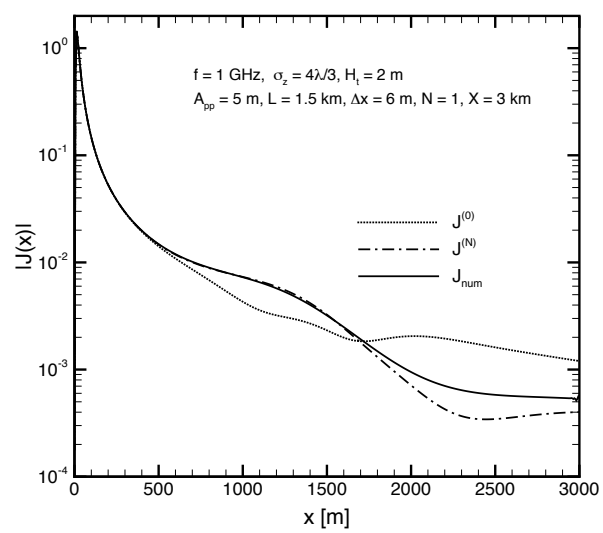

Fig. 6. Modulus of current density on a gaussian hill $g(x) = A_{pp}\exp(-(x-L)/\sigma_x^2)$.

seen that the zeroth order solution is indistinguishable from the numerical solution for ranges up to about 700 m, which roughly agrees with the estimate of $X_0 = 660\,\mathrm{m}$ from (59). The first order solution is virtually indistinguishable from the numerical solution over three orders of magnitude occurring for ranges up to about 1.6 km, that lies beyond the peak of the gaussian hill. The disagreement between the $N = 1$ series solution and the numerical solution is apparent only for small values of the current density. Even then, the propagation factor calculated with $J^{(1)}(x)$ as shown in Fig. 7 agrees very well with that obtained with the numerical solution.

We next consider the propagation of low-grazing angle waves over one realization of a fully-developed random sea surface. The surface is assumed to be zero mean and having Gaussian height statistics. As in [41], we model the roughness spectrum of the sea surface by the Pierson-Moskowitz (PM) spectrum, which is completely determined by the wind speed U flowing at a height of 19.5 m above the mean surface. The power spectral density $W(\kappa)$ for the PM spectrum as a function of the surface wavenumber κ is given by

$$W(\kappa) = \frac{\alpha}{4|\kappa|^3} e^{-3\kappa_p^2/2\kappa^2}, \tag{61}$$

where $\kappa_p = \sqrt{2\beta/3}\, g/U^2$ is the wave number at which the spectrum has a peak and $\alpha = 8.1\times 10^{-3}, \beta = 0.74, g = 9.81$ m/sec^2. The PM model provides a useful test of surface scattering theory with a range of roughness scales. Some useful parameters can be derived for the spectrum given in (61): the RMS surface height deviation, $\sigma_h = \sqrt{\alpha}/\sqrt{6}\kappa_p$ and the RMS correlation length of the surface $\rho_c = 5/2\sqrt{2}\kappa_p$. If the upper spatial wavenumber is truncated to κ_c, then the RMS slope of the surface $\sigma_{\mathrm{sl}} = \sqrt{\alpha E_1(y_c)}/2$, where $y_c = 3\kappa_p^2/2\kappa_c^2$ and $E_1(\cdot)$ is the exponential integral [37]. We generate a rough surface using

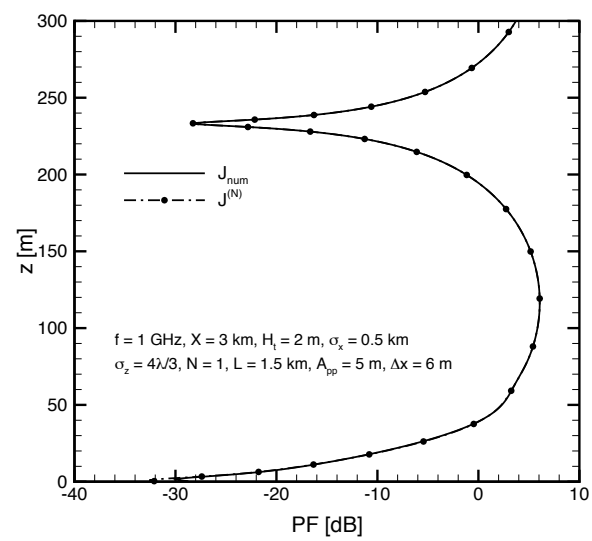

Fig. 7. Propagation factor at $X = 3\,\mathrm{km}$ for a gaussian hill $g(x) = A_{pp}\exp(-(x-L)/\sigma_x^2)$.

the spectral approach as outlined in [40], [42] for $U = 10\,\mathrm{m/s}$ and $\kappa_c = 51\kappa_p$ using a 512-point FFT. For this wind speed, $\sigma_h = 0.533\,\mathrm{m}$, $\rho_c = 25.7\,\mathrm{m}$. We generate a surface having an overall length of $X = 455\,\mathrm{m}$, so that $X/\rho_c \approx 17.7$. For the upper cutoff wavenumber chosen, $\sigma_{\mathrm{sl}} = 0.118$, while the maximum absolute slope of the surface is $\alpha_g = 0.139$, corresponding to a slope angle of 7.9^o. The generated surface is shown in Figure 8. We compute the zeroth order current density induced on this surface at a frequency of 1 GHz for the Gaussian source at a

height of $H_t = 2\,\mathrm{m}$ by (16) and compare it to the one generated numerically from solving (9). Figure 9 shows the comparison along with the other parameters used. It is seen that while the zeroth order approximation does not agree perfectly with the numerically generated one, it does follow the trends in various excursions rather accurately. Figure 10 shows a comparison of the corresponding propagation factors at the maximum range of 455 m. Very good agreement between the two is observed, despite the slight disagreement in the current distribution. It may be worth noting that the accuracy for the current distribution greatly improved by the use of the first order iterate $J^{(1)}(x)$ (not shown in the figures).

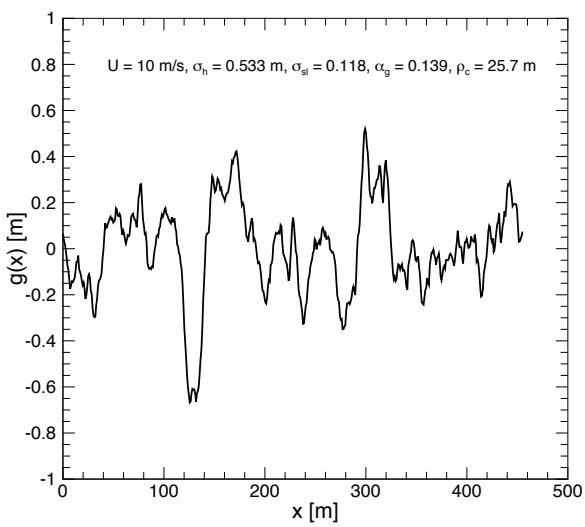

Fig. 8. A Pierson-Moskowitz sea surface for a wind speed of $U = 10\,\mathrm{m/s}$.

It is of interest to look at the computational times incurred in computing various approximations of the current density. Table I shows the CPU times involved in computing $J^{(0)}$, $J^{(N)}$, and J_{num} using MATLAB. We have made no attempt to optimize the various algorithmic steps involved in computing the current density by the Neumann series. The times shown for $J^{(N)}$ includes those spent in computing all of the previous orders $J^{(i)}$, $i = 1, \ldots, N-1$. Obviously, the time required to compute $J^{(0)}$ is a very small fraction of that required to compute J_{num}, because the former involves the computation of one integral. A good part of the time incurred in computing $J^{(N)}$ goes towards computing the kernel $K_1(x;t)$ in equation (17). Recall that $N = 5$ in Figure 4, while $N = 1$ in Figure 6. It is clear that the Neumann series solution will be very competitive in cases where only a few orders are adequate to accurately represent the current density. This, in turn, is dictated by the maximum slope of the surface and the maximum range involved.

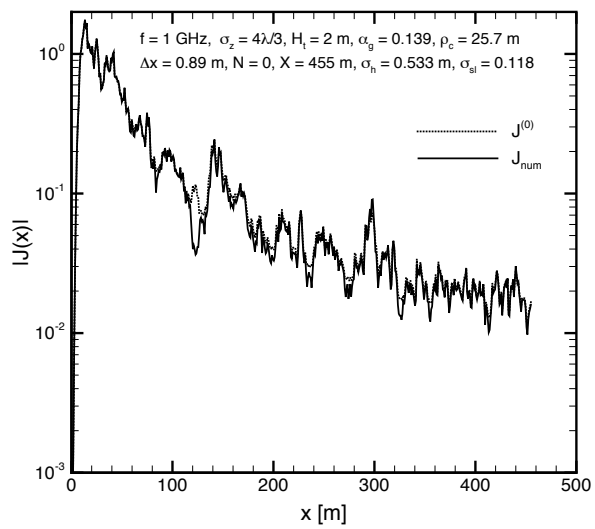

Fig. 9. Modulus of current density on a Pierson-Moskowitz rough surface.

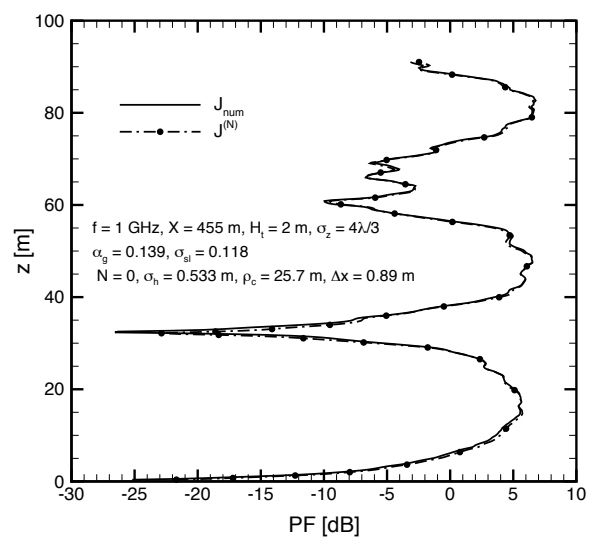

Fig. 10. Propagation factor at $X = 455\,\mathrm{m}$ for a Pierson-Moskowitz sea surface.

IV. Conclusion

A new Volterra integral equation of the second kind, (15), was derived for 2D wave propagation over a perfectly conducting rough surface and an exact expression, (27), was presented for the current density. The necessary and sufficient conditions for the exact series solution to converge were established: the rough surface should satisfy the uniform Lipschitz condition, (26), and the field at zero range should have finite first derivative

TABLE I
COMPUTATIONAL TIME (SEC) IN MATLAB

Current Density	Fig. 4	Fig. 6
$J^{(0)}$	0.1	0.2
$J^{(N)}$	101	48
J_{num}	73	50

with respect to height, (21). Because the formulation was based on the parabolic approximation to the Helmholtz equation, the exact solution presented is valid for low-grazing angle waves propagating over rough surfaces having gentle slopes when backscattering can be ignored. In practice, the solution should be valid for surfaces with absolute slope angles $\leq 10^o$. For a specified accuracy δ, equations (57) or (58) may be used to determine the number of terms needed in Neumann series representation. The number of terms used in the series is expected to increase with increasing range, increasing frequency of operation, and increasing slope angles. In order to keep the number of terms needed in the series to low values, the range should be restricted. However, this is not a serious limitation of the method. For, if propagation prediction is desired over long ranges, one can always employ the multiple-section strategy explored in [26], wherein the field calculated on a vertical line at the end of one short section serves as the initial field for the next section. An advantage of the series solution is that it provide complete error control, in that the number of terms can be chosen appropriately to achieve a certain relative error for the current distribution.

To make the series solution a viable and efficient numerical approach for studying wave propagation over rough surfaces, several algorithmic steps considered in the paper must be optimized. However, it is believed that the theory presented in the paper will lay the groundwork for obtaining approximate analytical solutions in a variety of situations. For instance, in low-grazing angle propagation over a sea surface, one is interested in the mean field at certain distance from the transmitter [1], [35], and [43]. This problem is also of interest to underwater acoustic propagation [27]. The importance of shadowing in low-grazing angle propagation has long been recognized, but is still an unresolved issue [44]. The current method incorporates all orders of shadowing interaction subject to the forward propagation approximation. The zeroth order approximation, (16), could be used in (5), as we have done in Figure 9, and the expectation performed with respect to the randomness of the sea surface to possibly yield an analytical solution for the total mean field when the maximum range of encompasses several correlation lengths of the random surface. The first term by itself, $J_i(x)$, in the zeroth order approximation will yield the well known Ament roughness reduction factor [10] for determining the mean field. This term will only incorporate the variance and mean of the rough surface. Correlation function of the rough surface will enter through the second term of $J^{(0)}(x)$ as well as through the higher order terms in the Neumann series. It is hoped that availability of such analytical expressions for the mean field will be useful in propagation modeling for radar detection [45] as well as wireless communications [42]. This will be explored in the future. Extension of the theory to surfaces modeled by the impedance boundary condition and to 3D propagation over 2D rough surfaces are worth exploring and these will be also be considered in the future.

ACKNOWLEDGEMENT

The above work was supported by the Army Research Office under grant ARO W911NF-10-1-0305.

REFERENCES

[1] W. S. Ament, "Towards a theory of reflection by a rough surface," *Proc. IRE*, vol. 41, no. 1, pp. 142–146, 1953.
[2] H. V. Hitney, J. H. Richter, R. A. Pappert, K. D. Anderson, and J. G. B. Baumgartnet, "Tropospheric radio propagation assessment," *Proc. IEEE*, vol. 73, no. 2, pp. 265–283, February 1985.
[3] F. T. Ulaby, R. K. Moore, and A. K. Fung, *Microwave Remote Sensing: Active and Passive*. Norwood: MA: Artech House, 1986, vol. II.
[4] L. Tsang, J. A. Kong, and K.-H. Ding, *Scattering of Electromagnetic Waves: Theories and Applications*. New York, NY: John Wiley & Sons, 2000.
[5] J. J. Egli, "Radio propagation above 40 mc over irregular terrain," *Proc. IRE*, vol. 45, no. 10, pp. 1383–1391, October 1957.
[6] A. G. Longley and P. L. Rice, "Prediction of troposhperic radio transmission loss over irregular terrain: A computer mthod-1968," Insititute for Telecommunication Services, Boulder, CO, Tech. Rept. AD0676874, July 1968.
[7] F. B. Jensen, W. A. Kuperman, M. B. Porter, and H. Schmidt, *Computational Ocean Acoustics*. New York, NY: Springer-Verlag, 2000.
[8] J. M. Elson, "Theory of light scattering from a rough surface with an inhomogeneous dielectric permittivity," *Physical Review B*, vol. 30, no. 10, pp. 5460–5480, November 1984.
[9] A. Ishimaru, *Wave Propagation and Scattering in Random Media*. Piscataway, NJ: IEEE Press, 1997.
[10] P. Beckmann and A. Spizzichino, *The Scattering of Electromagnetic Waves from Rough Surfaces*. New York, NY: Pergamon Press, 1963.
[11] G. S. Brown, "Application of the integral equation method of smoothing to random surface scattering," *IEEE Transactions Antennas Propagat.*, vol. 32, no. 12, pp. 1308–12 312, December 1984.
[12] D. Holliday, "Resolution of a controversy surrounding the Kirchoff approach and the small perturbation method in rough surface scattering," *IEEE Transactions Antennas Propagat.*, vol. 35, no. 1, pp. 120–122, January 1987.
[13] R. Janaswamy, "A Fredholm integral equation method for propagation predictions over small terrain irregularities," *IEEE Transactions Antennas Propagat.*, vol. 40, no. 11, pp. 1416–1422, November 1992.
[14] J. T. Hviid, J. B. Andersen, J. Toftgard, and J. Bojer, "Terrain-based propagation model for rural area-an integral equation approach," *IEEE Transactions Antennas Propagat.*, vol. 43, no. 1, pp. 41–46, January 1995.
[15] L. Tsang, J. A. Kong, and K.-H. Ding, *Scattering of Electromagnetic Waves: Advanced Topics*. New York, NY: John Wiley & Sons, 2001.
[16] R. Petit, *Electromagnetic Theory of Gratings*, ser. Topics in current physics, v. 22. New York, NY: Springer-Verlag, 1980.
[17] D. E. Barrick, "Grazing behavior of scatter and propagation above any rough surface," *IEEE Transactions Antennas Propagat.*, vol. 46, no. 1, pp. 73–83, 1998.
[18] A. E. Barrios, "A terrain parabolic equation model for propagation in the troposphere," *IEEE Transactions Antennas Propagat.*, vol. 42, no. 1, pp. 90–98, January 1994.
[19] S. W. Marcus, "A hybrid (finite-difference-surface Green's function) method for computing transmission losses in an inhomogeneous atmosphere over irregular terrain," *IEEE Transactions Antennas Propagat.*, vol. 40, no. 12, pp. 1451–1459, December 1002.
[20] R. Janaswamy, "A fast finite difference method for propagation predictions over irregular, inhomogeneous terrain," *IEEE Transactions Antennas Propagat.*, vol. 42, no. 9, pp. 1257–1267, September 1994.
[21] V. A. Fock, *Electromagnetic diffraction and propagation problems*. New York, NY: Pergamon Press, 1965.

[22] M. F. Levy, *Parabolic Equation Methods for Electromagnetic Wave Propagation*, ser. Electromagnetic Wave Series, v. 45. London: UK: IEE Press, 2000.

[23] J. V. Roey, J. van der Donk, and P. E. Lagasse, "Beam-propagation method: analysis and assessment," *J. Opt. Soc. Am.*, vol. 71, no. 7, pp. 803–810, 1981.

[24] G. A. Hufford, "An integral equation approach to the problem of wave propagation over an irregular surface," *Quarterly Appl. Math.*, vol. 9, no. 4, pp. 391–404, 1952.

[25] R. H. Ott, "An alternative integral equation for propagation over irregular terrain, 2," *Radio Science*, vol. 6, no. 4, pp. 429–435, April 1971.

[26] M. J. Motta, "Equivalent impedance of rough surface at low grazing angles," (Available online at http://www.dtic.mil/cgi-bin/GetTRDoc?AD=ADA369420.), Naval Postgraduate School, Monterey, CA, September 1999.

[27] B. J. Uscinski and C. J. Stanek, "Acoustic scattering from a rough sea surface: the mean field by the integral equation method," *Waves in Random Media*, vol. 12, pp. 247–263, 2002.

[28] D. Holliday, J. L. L. DeRaad, and G. J. St-Cyr, "Volterra approximation for low grazing angle shadowing on smooth ocean-like surfaces," *IEEE Transactions Antennas Propagat.*, vol. 43, no. 11, pp. 1199–1207, November 1995.

[29] E. Kreyszig, *Introductory Functional Analysis with Applications*, ser. Wiley Classics Library. New York, NY: John Wiley & Sons, 1978.

[30] W. C. Jakes, Ed., *Microwave Mobile Communications*. Piscataway, NJ: IEEE Press, 1974.

[31] D. Parsons, *The Mobile Radio Propagation Channel, D. Parsons, London, U.K.: Pentech Press, 1992*. London: UK: Pentech Press, 1992.

[32] J. R. Kuttler and G. D. Dockery, "Theoretical description of the parabolic approximation/Fourier split-step method of representing electromagnetic propagation in the troposphere," *Radio Science*, vol. 26, no. 2, pp. 381–393, March-April 1991.

[33] R. Janaswamy, "Roadiowave propagation over a nonconstant immittance plane," *Radio Science*, vol. 36, no. 3, pp. 387–405, May-June 2001.

[34] B. Davies, *Integral Transforms and Their Applications*, 3rd ed. New York, NY: Springer-Verlag, 2002.

[35] Z. Lai and R. Janaswamy, "Specular propagation over rough surfaces: numerical assessment of Uscinski and Stanek's mean Green's function technique," *Waves in Random and Complex Media*, vol. 16, no. 2, pp. 137–150, May 2006.

[36] F. G. Tricomi, *Integral Equations*, ser. Wiley Interscience. New York, NY: John Wiley & Sons, 1957.

[37] M. Abramowitz and I. A. Stegun, Eds., *Handbook of Mathematical Functions: with Formulas, Graphs, and Mathematical Tables*. New York, NY: Dover, 1964.

[38] L. Debnath and P. Mikusinski, *Introduction to Hilbert Spaces with Applications*, 2nd ed. New York, NY: Academic Press, 1999.

[39] N. M. Temme, "Uniform asymptotics for the incomplete gamma functions starting from negative values of the parameters," *Methods and Applications of Analysis*, vol. 3, no. 3, pp. 335–344, 1996.

[40] E. I. Thorsos, "The validity of the Kirchoff approximation for a rough surface scattering using a Gaussian roughness spectrum," *J. Acoustical Soc. America*, vol. 83, no. 1, pp. 78–92, January 1988.

[41] ——, "Acoustic scattering from a "Pierson-Moskowitz" sea surface," *J. Acoustical Soc. America*, vol. 88, no. 1, pp. 335–349, July 1990.

[42] R. Janaswamy, *Radiowave Propagation and Smart Antennas for Wireless Communications*. Norwell: MA: Kluwer Academic Publishers, 2001.

[43] D. E. Freund, N. E. Woods, H.-C. Ku, and R. S. Awadallah, "Forward radar propagation over a rough sea surface: A numerical assessment of the Miller-Brown approximation using a horizontally polarized 3-GHz line source," *IEEE Transactions Antennas Propagat.*, vol. 54, no. 4, pp. 1292–1304, April 2006.

[44] ——, "The effect of shadowing on modelling forward radar propagation over a rough sea surface," *Waves in Random and Complex Media*, vol. 18, no. 3, pp. 387–408, August 2008.

[45] A. Karimian, C. Yardim, P. Gerstoft, W. S. Hodgkiss, and A. E. Barrios, "Multiple grazing angle sea clutter modeling," *IEEE Transactions Antennas Propagat.*, vol. 60, no. 9, pp. 4408–4417, September 2012.